Materials Science and Engineering C 29 (2009) 140–143

Contents lists available at ScienceDirect

Materials Science and Engineering C

journal homepage: www.elsevier.com/locate/msec

Characterisation and optical vapour sensing properties of PMMA thin films

İ. Çapan [a,*], Ç. Tarımcı [b], A.K. Hassan [c], T. Tanrısever [d]

[a] Balikesir University, Science and Arts Faculty, Physics Department, 10100 Balikesir, Turkey
[b] Ankara University, Faculty of Engineering, Department of Engineering Physics, 06100, Tandoğan, Ankara, Turkey
[c] Sheffield Hallam University, Materials and Engineering Research Institute, City Campus, Pond Street, Sheffield S1 1WB, UK
[d] Balikesir University, Science and Arts Faculty, Chemistry Department, 10100 Balikesir, Turkey

ARTICLE INFO

Article history:
Received 14 February 2008
Received in revised form 29 April 2008
Accepted 31 May 2008
Available online 12 June 2008

Keywords:
PMMA
Organic vapour sensing
SPR

ABSTRACT

The present article reports on the characterisation of spin coated thin films of poly (methyl methacrylate) (PMMA) for their use in organic vapour sensing application. Thin film properties of PMMA are studied by UV–visible spectroscopy, atomic force microscopy and surface plasmon resonance (SPR) technique. Results obtained show that homogeneous thin films with thickness in the range between 6 and 15 nm have been successfully prepared when films were spun at speeds between 1000–5000 rpm. Using SPR technique, the sensing properties of the spun films were studied on exposures to several halohydrocarbons including chloroform, dichloromethane and trichloroethylene. Data from measured kinetic response have been used to evaluate the sensitivity of the studied films to the various analyte molecules in terms of normalised response (%) per unit concentration (ppm). The highest PMMA film sensitivity of 0.067 normalised response per ppm was observed for chloroform vapour, for films spun at 1000 rpm. The high film's sensitivity to chloroform vapour was ascribed mainly to its solubility parameter and molar volume values. Effect of film thickness on the vapour sensing properties is also discussed.

1. Introduction

The volatile organic compounds (VOCs) are detected in environment as a result of their extensive use in industrial and commercial applications. They are toxic and carcinogenic for human health. Volatile halohydrocarbons (VHHs) is one of the most dangerous classes of VOCs which are the most ubiquitous in human living. Detection of these gases in atmosphere has become an important environmental issue [1–3]. Extensive studies have been carried out using different monitoring techniques such as gravimetric [4–7], electrical [8] and optical techniques [9–11]. Surface plasmon resonance (SPR), is an optical technique that measures changes in thin films optical parameters during interaction with various toxic gases. Changes in optical parameters of the thin film during exposure to toxic gases can be monitored on-line. High sensitivity and selectivity have been obtained using this technique [12–14].

In gas sensing applications one of the most important parameters is the sensing layer which produces a signal during exposure to a toxic gas. In the last decade polymeric thin films have attracted interest for gas sensing applications because of their high sensitivity and selectivity [15,16]. PMMA is one of the most studied polymers owing to its long-term stability [17], low-cost, low optical loss in the visible spectrum, high scratch hardness and low glass temperature [18,19]. Optical, electrical and microgravimetric properties of PMMA thin films were used to investigate the chemical sensing capability. It has been found that PMMA thin films were sensitive to several VOCs including xylene and toluene with the detection limits in the range of ppm [20,21]. Mixed thin films of chemically modified multi-walled carbon nanotubes (MWCNTs) and poly(methylmethacrylate) (PMMA) thin films were also sensitive to methanol and ammonia vapors with very short response and recovery times in the range of a few seconds which was believed to be a result of semiconducting properties of MWCNTs [22].

In this work characterisation of thin films of PMMA has been studied using UV–Visible spectroscopy and AFM. Gas sensing properties of the PMMA films has been investigated using SPR method. The sensitivity of the films was calculated and effects of the various parameters, such as film thickness on gas sensing properties have been discussed.

2. Experimental details

Poly(methyl methacrylate) molecules with different molecular weights have been synthesised using emulsifier-free emulsion polymerization method. The synthesis, physical and chemical properties of PMMA molecules have previously been reported in detail [23] and the chemical structure was given elsewhere [24]. PMMA used in this work has a molecular weight of 1200 kg mol^{-1} and average

* Corresponding author. Tel.: +90 266 612 1000; fax: +90 266 612 12 15.
E-mail address: inci.capan@gmail.com (İ. Çapan).

0928-4931/$ – see front matter © 2008 Elsevier B.V. All rights reserved.
doi:10.1016/j.msec.2008.05.021

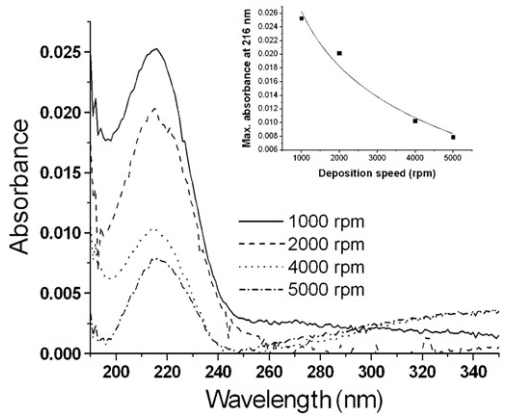

Fig. 1. UV–Visible spectra of spun PMMA thin films. The relation between maximum absorbance at λ=216 mm and spin speed is given in the inset.

particle diameters of 0.14 μm. Three different analytes; chloroform ($CHCl_3$), dichloromethane (DCM) (CH_2Cl_2) and trichloroethylene (TCE) ($CHCl_2$:CCl_2) were purchased from Acros Chemicals, Aristar and J. Preston LTD., respectively and used without further purification.

Using chloroform as solvent, solutions of PMMA molecules were prepared with the concentrations in the range 2–10 mg ml^{-1}. These solutions were used to obtain thin films via spin coating technique. For SPR measurements a thin layer of gold (around 50 nm thick) was thermally evaporated onto pre-cleaned glass substrates using Edwards E306A vacuum coating unit, with deposition rate kept at 0.2 nm s^{-1} under vacuum better than 2×10^{-3} Pa. Using an Electronic Microsystems spin-coating unit (Model 4000), 100 μl of solution was dispensed onto ultrasonically cleaned glass substrate which was rotating at a fixed deposition spin speed for 30 s and then allowed another 30 s for the thin film to dry. The experimental optical set-up for SPR measurements based on Kretschmann's configuration [25] which was introduced elsewhere [26,27] is used in the current work. The thin film coated slides were brought into optical contact with the semi-cylindrical prism (with a refractive index of 1.515) using ethyl salicylate, 99% (Aldrich) as an index matching fluid. P-polarised beam with the wavelength of 632.8 nm was obtained using a He–Ne laser source for the excitation of surface plasmons.

UV–Visible measurements have been carried out using a Varian (Cary 50) UV–Visible spectrophotometer operating in the spectral range of 180–900 nm. Surface morphology of spin coated PMMA films were investigated by using atomic force microscopy (Nanoscope IIIa instrument). For Atomic Force Microscopy (AFM) and UV–Visible spectrometer measurements, thin films of PMMA molecules were spun onto 0.3 mm thick silicon substrates and quartz slides respectively using the same technique described above.

For gas sensing experiments a poly (tetrafluoro ethylene) (PTFE) gas cell with a rubber O-ring sealed by the coated slides was used. Chloroform, DCM and TCE vapours which were mixed with dry air at various concentrations have been injected into the gas cell using a 10 ml syringe. Kinetic response of thin films to repeated exposures of analyte vapours were performed at room temperature where reflected light intensity was measured as a function of time at a fixed angle θ^* which was chosen near the minimum on the left-hand side of the SPR curve.

3. Results and discussion

3.1. Characterisation of spin coated PMMA films

Thin films of PMMA molecules were spun at different speeds in the range 1000–5000 rpm and used for this investigation. Fig. 1 shows the UV–Visible spectra of PMMA films deposited onto quartz glass substrates at different spin speeds. The maximum absorbance occurring at 216 nm [28] is found to decrease as a result of decreasing film thickness with increased spin speed. This is the main characteristic absorption peak for PMMA, and variation observed in the spectral region around 340 nm of the absorption spectra in the case of thinner PMMA films are probably associated with noise, most likely due to film thinness. The main spectral characteristics of all measured curves are retained irrespective of film spinning speed (ω). The inset to Fig. 1 shows the monotonic decrease in film thickness with increased deposition speed at the main absorption band at 216 nm. This dependence correlates well with the inverse proportionality between film thickness and the spin speed which is expressed by the relation $d\sim\omega^{-n}$ [29], where d is the film thickness and ω is the deposition spin speed.

Fig. 2 shows an AFM image of a PMMA thin film spun onto silicon substrate at 2000 rpm. Randomly scattered pores with an average diameter of 61 nm and an average depth of 6 nm have been observed. The pore density was calculated to be 8.8×10^{12} m^{-2}. The rms value of film roughness was estimated as 1.7 nm.

3.2. SPR curves consideration

SPR curves were produced by measuring reflected light intensity as a function of the angle of incidence θ in the range 39°–49° at the interface between the glass prism and the metal/PMMA layer structure. The minimum value of reflectance which corresponds to the surface plasmon resonance angle (θ_{SPR}) shows a shift ($\Delta\theta$) in the presence of a spun PMMA film on gold layer compared to the SPR curve of the bare gold film, as well as a further shift when PMMA film is exposed to the various chemical vapours. $\Delta\theta$ is given by the following expression [30]

$$\Delta\theta = \frac{(2\pi/\lambda)(|\varepsilon_m|\varepsilon_i)^{3/2}d}{n_p\cos\theta(|\varepsilon_m|-\varepsilon_i)^2\varepsilon}(\varepsilon-\varepsilon_i) \quad (1)$$

where λ is the wavelength of the He–Ne laser beam, n_p is the refractive index of the semi-cylindrical prism, $|\varepsilon_m|$ is the modulus of the complex dielectric constant of the gold film and ε_i is the dielectric constant of the medium in contact with the spun PMMA thin film. Using this equation dielectric constant ε and thickness d of spun PMMA thin films can be evaluated.

Fig. 3 shows SPR curves obtained for glass/gold/spun PMMA film/air system (curve a), the same system during exposure to saturated vapour of TCE (curve b) and SPR curve of the system after the gas cell

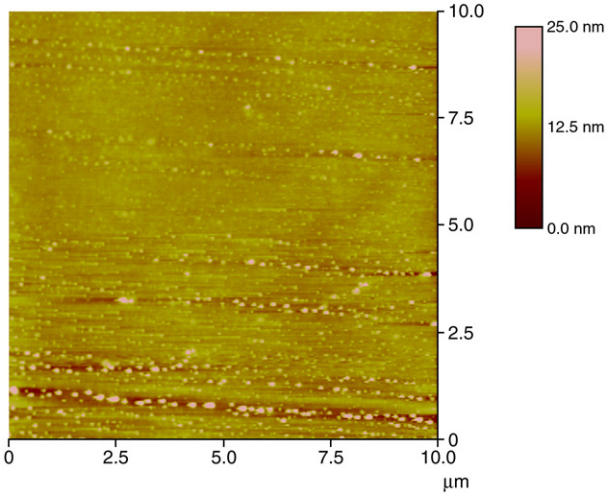

Fig. 2. 2D AFM image of a PMMA thin film spun at deposition speed of 2000 rpm.

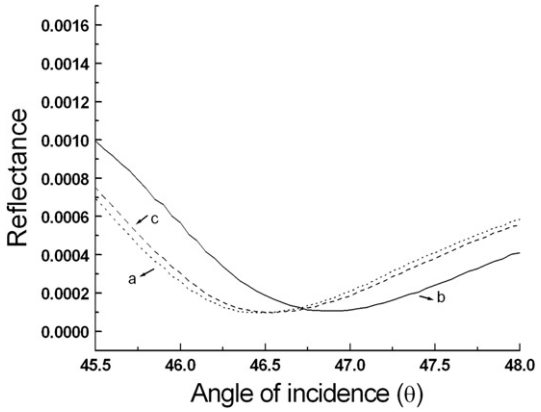

Fig. 3. SPR curves measured for a freshly spun PMMA films (a), during exposure to saturated vapor of TCE (b), and post-recovery on purging the gas cell with dry air (c).

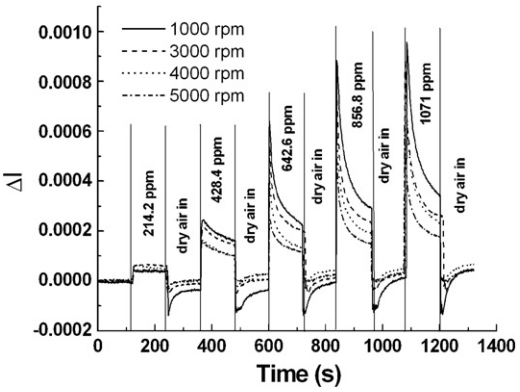

Fig. 4. The change in reflected light intensity, Δ*I*, of spun PMMA films as a function of exposure time to chloroform vapor.

was purged with dry air (curve c). The three SPR curve measurements were performed on a PMMA film prepared with a spin speed of 4000 rpm. Injection of saturated vapor causes the resonance angle θ_{SPR} to shift to larger angles, and a $\Delta\theta_{SPR}=0.28°$ has been observed between the SPR curves of the freshly prepared film and that measured during exposure of the same film to TCE. The resonance angle θ_{SPR} for the post-recovery curve was 45.29° which is very close to $\theta_{SPR}=45.18°$ of the fresh sample, indicating a reasonably good recovery. Any deviation from complete recovery may be understood in terms of residual vapour molecules physically adsorbing to the PMMA film surface as a result of flushing the gas cell by injecting clean air using a syringe. Full recovery however is expected to occur if the gas cell can be flushed with a continuous flow of dry air.

The injection of chloroform and DCM into the gas cell was found to cause similar changes in the resonance angles of the measured SPR curves. The refractive index values of the studied analytes are 1.443, 1.424 and 1.485 for chloroform, DCM and TCE respectively [31], while that of PMMA film is 1.4887 [32,33]. It was therefore assumed that the refractive index of PMMA film will remain unchanged as a result of interaction with the analytes' saturated vapour, due to the close similarity between refractive index values of solvents and PMMA film. Vapour interaction with the PMMA film is therefore expected to mainly increase the film thickness as a result of film swelling. Swelling however is expected to alter film density and may therefore lead to a change in the film refractive index. The overall change in film refractive index is therefore expected to be negligibly small. Changes in the thickness of the vapour-treated films have been determined by performing numerical solution of the experimental SPR data using Eq. (1). In order to accurately evaluate such changes in film thickness we have assumed an extinction coefficient value of zero, since PMMA films are transparent to the wavelength $\lambda=632.8$ nm which is used for surface plasmon excitation. Table 1 presents the calculated values of film thickness which clearly shows that change in film thickness (Δd) is increasing as a result of vapour exposure, especially in the case of exposures to chloroform and DCM. Furthermore, data in Table 1 shows that Δd is clearly decreasing as the film thickness is decreasing, again with the exception of films exposed to TCE, as well as in the case of PMMA film of the highest thickness on exposure to chloroform. The latter may be explained in terms of the effect of residual chloroform molecules which remained trapped inside the film matrix due to incomplete drying after film fabrication. The presence of such molecules is expected to reduce the film response to vapour exposures of the same solvent molecules, and this effect is believed to be more pronounced for thicker films.

Table 1
Thickness values *d* (nm) of spun PMMA films before exposure and the change in thickness due to the interaction between the thin film and the gas molecules Δ*d* (nm) obtained by fitting of SPR curves

Deposition spin speed	Thickness (nm)					
	Chloroform		DCM		TCE	
	d	Δ*d*	*d*	Δ*d*	*d*	Δ*d*
1000 rpm	15.24	2.07	12.92	3.7	15.24	0.42
3000 rpm	9.03	2.69	9.58	1.51	9.86	0.55
4000 rpm	6.85	1.93	7.76	1.3	7.84	0.42
5000 rpm	6.39	1.26	–	–	–	–

3.3. Kinetic response measurements using SPR set-up

Fig. 4 shows the kinetic response in terms of the change in reflected light intensity Δ*I* versus exposure time, when PMMA film was exposed to chloroform in the concentration range 0–1100 ppm. Exposure of PMMA films to chloroform vapour for 2 min was followed by 2 min recovery by purging the gas cell with dry air. Similar trends of responses were obtained for experiments performed with DCM and TCE vapour exposures. The variations in the baseline have been attributed to a combination of factors including experimental errors, relatively poor stability of the He–Ne laser and substrate cooling effect [34]. The interaction of the thin film with analyte molecules is believed to be occurring in two stages; The first stage is a result of the adsorption/condensation of analyte gas molecules forming a wet layer onto the film surface which causes a sharp increase in the reflected light intensity; this is followed by the second stage where the vapour molecules penetrate into the film matrix causing film swelling and thus increased film thickness [26]. A smaller kinetic response was also observed for thinner films fabricated with higher spin speeds. Similar

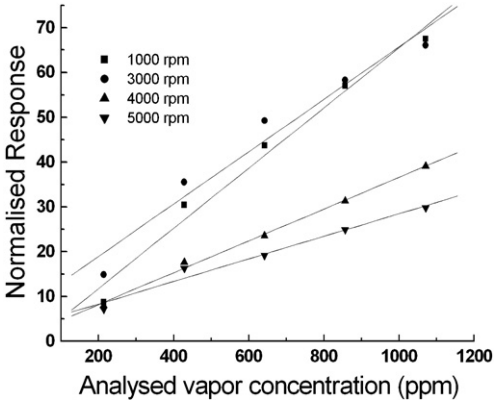

Fig. 5. Calibration curves obtained using dynamic response plots for DCM vapor at different concentrations.

Table 2
The sensitivity of the sensors in terms of normalised response per concentration at different film deposition spin speeds

Slope of the calibration curves for different deposition spin speed (normalised response/ppm)					
Analytes	1000 rpm	2000 rpm	3000 rpm	4000 rpm	5000 rpm
Chloroform	0.067	0.058	0.058	0.035	0.025
DCM	0.039	0.018	0.022	0.016	0.018
TCE	0.036	0.024	0.039	0.027	0.017

behaviour has been previously observed for various other chemical detection systems [35,36]. It is believed that with increasing film thickness the swelling of the films becomes more important because of the bulk diffusion into the thin film structure [36].

The kinetic response data given in Fig. 4 representing exposures of PMMA films spun at different speeds have been used to calculate the normalised response of PMMA film on exposures to chloroform vapour with the help of the following equation:

$$\frac{\Delta R}{R} = \frac{R_{gas} - R_{air}}{R_{air}} \times 100 \quad (2)$$

where R_{gas} and R_{air} represents the measured reflectance values of PMMA film during exposures to the analyte vapour and at the time of flushing with dry air, respectively using the nearly flat parts of the kinetic response curves.

Fig. 5 shows a plot of the normalised response as a function of DCM vapour concentration. The response of the PMMA films is shown to be approximately linear with the concentration in the investigated range, suggesting a bulk absorption in the film [37]. The slope of the calibration curves of all investigated organic vapours, which represents the sensitivity, have been summarised in Table 2 in terms of normalised response per unit concentration (ppm). The highest sensitivity is clearly associated with the largest studied film thickness for all analytes, and the best sensitivity has been observed for chloroform vapour. Sensitivity values of 0.067, 0.039 and 0.036 normalised response/ppm for chloroform, DCM and TCE vapours respectively, were obtained for the film spun at 1000 rpm. These results were estimated by performing linear curve fitting to the obtained sensitivity values calculated from Eq. (2). All calculated values have been listed in Table 2.

The mechanism of interaction between chloroform, DCM and TCE vapours and the PMMA film may be described in terms of different mechanisms which are governed by parameters such as solubility and molar volume of the vapour molecules. The response will be largely determined by the solubility of vapour molecules in the film matrix if molecules of both materials have high dipole moment [38]. The solubility parameter value of PMMA (18.6 $MPa^{1/2}$) which is very close to those of chloroform and TCE (both having a value of 18.7 $MPa^{1/2}$) explains the relatively good response of PMMA film to chloroform and TCE vapours [39–42] compared to the PMMA film's response to DCM with solubility parameter 20.2 $MPa^{1/2}$. During the second stage of the film response to the analytes, where vapour molecules are diffusing into the film structure, high molecular volume of analyte molecules is expected to hinder this process [43]. The lowest sensitivity was observed for TCE vapour exposures, which may be associated with the highest molar volume of its molecules. This mechanism is expected to be more pronounced with increasing film thickness [26], as was pointed out earlier on.

4. Conclusion

It has been demonstrated that spun films of PMMA polymer can potentially be used as an element in the optical detection of halohydrocarbons. Thin films of PMMA were exposed to different concentrations of chloroform, dichloromethane and trichloroethylene, using surface plasmon resonance as the optical detection method. High sensitivity to DCM was mainly ascribed to the smaller volume of the analyte molecules, which was found to aide the diffusion of the vapour molecules into the film matrix resulting in film swelling and thus increased film thickness. The latter is shown to be the major factor for the observed SPR resonance shift. Other physical parameters of the analyte molecules, including solubility and molar volume are also shown to influence the gas sensing properties of the PMMA films. Furthermore, it has been argued that increased response of PMMA films to exposures of chloroform and DCM becomes more pronounced with increased film thickness.

References

[1] Y. Li, T. Zhang, P. Liang, Anal. Chim. Acta 536 (2005) 245.
[2] A. Lua, J. Liu, D. Zhao, Y. Guo, Q. Li, N. Li, Catal. Today 90 (2004) 337.
[3] M.H. China, C.C. Liu, T.C. Chou, Biosens. Bioelectron. 20 (2004) 25.
[4] R. Ni, X.B. Zhang, W. Liu, G. Li Shen, R.Q. Yu, Sens. Actuators, B, Chem. 88 (2003) 198.
[5] R.A. Potyrailo, T.M. Sivavec, Sens. Actuators, B, Chem. 106 (2005) 249.
[6] A. Mirmohseni, K. Rostamizadeh, Sensors 6 (2006) 324.
[7] I.A. Koshets, Z.I. Kazantseva, Yu, M. Shirshov, S.A. Cherenok, V.I. Kalchenko, Sens. Actuators, B, Chem. 106 (2005) 177.
[8] K.I. Arshak, L.M. Cavanagh, E.G. Moore, Mater. Sci. Eng. C 26 (2006) 1032.
[9] M. Akrajas, M. Saleh, M. Yahaya, Sens. Actuators, B, Chem. 85 (2002) 191.
[10] A.V. Nabok, F. Davis, A.K. Hassan, A.K. Ray, R. Majeed, Z. Ghassemlooy, Mater. Sci. Eng. C 8–9 (1999) 123.
[11] T.H. Richardson, C.M. Dooling, L.T. Jones, R.A. Brook, Adv. Colloid Interface Sci. 116 (2005) 81.
[12] R. Casalini, J.N. Wilde, J. Nagel, U. Oertel, M.C. Petty, Sens. Actuators, B, Chem. 57 (1999) 28.
[13] A.K. Hassan, A.K. Ray, A.V. Nabok, T. Wilkop, Appl. Surf. Sci. 182 (2001) 49.
[14] E.B. Feresenbet, E. Dalcanale, C. Dulcey, D.K. Shenoy, Sens. Actuators, B, Chem. 97 (2004) 211.
[15] B. Adhikari, S. Majumdar, Prog. Polym. Sci. 29 (2004) 699.
[16] D.N. Debarnot, F.P. Epaillard, Anal. Chim. Acta 475 (2003) 1.
[17] D.Y. Sasaki, S. Singh, J.D. Cox, P.I. Pohl, Sens. Actuators, B, Chem. 72 (2001) 51.
[18] T.M. Long, S. Prakash, M.A. Shannon, J.S. Moore, Langmuir 22 (2006) 4104.
[19] Y. Li, H. Wang, M. Yang, Sens. Actuators, B, Chem. 121 (2007) 496.
[20] M. Matsuguchi, T. Uno, Sens. Actuators, B, Chem. 113 (2006) 94.
[21] O.V. Vassiltsova, Z. Zhao, M.A. Petrukhina, M.A. Carpenter, Sens. Actuators, B, Chem. 123 (2007) 522.
[22] Yang Li, Hui-cai Wang, Mu-jie Yang, Sens. Actuators, B, Chem. 121 (2007) 496.
[23] T. Tanrisever, O. Okay, I.Ç. Sonmezoglu, J. Appl. Polym. Sci 61 (1996) 485.
[24] I. Çapan, R. Çapan, T. Tanrisever, S. Can, Mater. Lett. 59 (2005) 2468.
[25] E. Kretschmann, H. Raether, Z. Naturforsch. 23A (1968) 2135.
[26] A.V. Nabok, A.K. Hassan, A.K. Ray, O. Omar, V.I. Kalchenko, Sens. Actuators, B, Chem. 45 (1997) 115.
[27] R. Çapan, A.K. Ray, T. Tanrısever, A.K. Hassan, Smart Mater. Struct. 14 (2005) N1–N5.
[28] R. Srinivasan, B. Braren, K.G. Casey, Pure Appl. Chem. 62 (1990) 1581.
[29] B. Torriero, M.L. Pourcel-Gouzy, I. Gumenyuk, J.B. Doucet, A. Martinez, P. Temple-Boyer, Microelectron. J. 37 (2006) 133.
[30] I. Pockrand, Surf. Sci. 72 (1978) 577.
[31] S. Valkai, J. Liszi, I. Szalai, J. Chem. Thermodyn. 30 (1998) 825.
[32] C.B. Walsh, E.I. Franses, Thin Solid Films 347 (1999) 167.
[33] C.B. Walsh, E.I. Franses, Thin Solid Films 429 (2003) 71.
[34] J.N. Wilde, J. Nagel, M.C. Petty, Thin Solid Films 327–329 (1998) 726.
[35] H.J. Nam, T. Sasaki, N. Hoshizaki, J. Phys. Chem. C 111 (2007) 9105.
[36] Y.L. Lee, C.Y. Sheu, R.H. Hsiao, Sens. Actuators, B, Chem. 99 (2004) 281.
[37] A.F. Holloway, A. Nabok, M. Thompson, A.K. Ray, D. Crowther, J. Siddiqi, Sensors 3 (2003) 187.
[38] B.C. Sih, M.O. Wolf, D. Jarvis, J.F. Young, J. Appl. Phys. 98 (2005) 114314.
[39] J. Liu, T. Liu, S. Kumar, Polymer 46 (2005) 3419.
[40] J. Jaczewska, I. Raptis, A. Budkowski, D. Goustouridis, J. Raczkowska, M. Sanopoulou, E. Pamuła, A. Bernasik, J. Rysz, Synth. Met. 157 (2007) 726.
[41] Y.H. Lang, Z.M. Cao, X. Jiang, Talanta 66 (2005) 249.
[42] S. Song, D.Y. Kang, M.J. Kim, J.E. Park, H.H. Lee, J. Membr. Sci. 305 (2007) 5.
[43] W. Zeng, M.Q. Zhang, M.Z. Rong, Q. Zheng, Sens. Actuators, B, Chem. 124 (2007) 118.